Multi-model trends in the Sahara induced by increasing CO_2

Ping Liu

International Pacific Research Center, University of Hawaii, Honolulu

Gerald A. Meehl

National Center for Atmospheric Research, Boulder, Colorado

Guoxiong Wu

Laboratory of Atmospheric Sciences and Geophysical Fluid Dynamics,

Institute of Atmospheric Physics, Beijing, China

P. Liu, International Pacific Research Center, University of Hawaii, Honolulu, HI 96822. (e-mail: pliu@hawaii.edu)

G. A. Meehl, National Center for Atmospheric Research (NCAR), P.O. Box 3000, Boulder, CO 80307. (e-mail: meehl@ucar.edu)

G. Wu, Laboratory of Atmospheric Sciences and Geophysical Fluid Dynamics, Institute of Atmoshperic Physics, P.O. Box 9804, Beijing 100029, China. (e-mail: gxwu@lasg.iap.ac.cn)

Abstract.

Five of eighteen climate system models participating the Coupled Model Intercomparison Project (CMIP) are chosen here for analysis based on their ability to simulate a reasonable present-day climatology of the Sahara Desert with similar rainfall distributions and meridional boundaries as in the observational data. When CO_2 concentration is increased at one percent per year for 80 years in these models the Sahara moves north, becomes hotter and dries. Compared to the 40-year control run climatology, the mean average northward shift is around 0.55°latitude and the surface temperature is about 1.8°C warmer at year 70 when the CO_2 doubles. The local enhanced greenhouse effect from increased CO_2 increases the net surface sensible heat flux, which in turn contributes to the warming trend.

1. Introduction

The Sahara Desert has been getting wetter, then drier, and contracting northward, then expanding southward, from the distant past to the 20^{th} century [*Maley*, 1977; *Dumont*, 1978; *Ritchie et al.*, 1985; *Gasse et al.*, 1990]. The southern boundary underwent a series of decade long droughts before the 1970s [*Klaus*, 1978; *Littmann*, 1991] without an established trend or periodicity in the western region [*Bunting*, 1976]. The 1980s brought an apparent expansion and an increase in interannual variations [*Tucker et al.*, 1991]. A warming, drying, shrinking and northward retreating Sahara is seen in a projection of 21^{st} century climate change in a global coupled climate model [*Liu et al.*, 2001b] (Liu2001 hereafter).

The southern Sahara Desert may be sustained through a biogeophysical feedback mechanism [*Charney et al.*, 1975; *Zeng et al.*, 1999]. Changes of albedo and roughness from reduced vegetation cover modify the net radiative flux at the surface and cause further desertification. Other processes, such as large scale circulation [*Wolter*, 1989], sea temperature [*Palmer*, 1986], ITCZ [*Greenhut*, 1981] associated with local meridional circulation change [*Liu et al.*, 2001a], and greenhouse gas emissions (Liu2001) could affect the rainfall and temperature over the Sahara Desert. Since none of the models in the present study have interactive vegetation schemes, only the latter processes are considered here.

Eighteen climate models participating the Coupled Model Intercomparison Project (CMIP) [*Meehl et al.*, 2000] carry out integrations to evaluate the effects of increasing CO_2 on global climate [*Covey et al.*, 2001]. Five models are chosen for analysis here based on their ability to simulate a reasonable dry modern climatology in the Sahara Desert (including the Parallel Climate Model (PCM) [*Washington*, 2000] analyzed earlier

in Liu2001) and are compared with observational data. In the scenario of CO_2 increasing one percent per year, we will show these models predict a warming, drying and northward retreating Sahara Desert in agreement with the PCM in Liu2001. As was the case for the PCM, we will show for these models with increased CO_2 a reduction of the net longwave radiation flux from the earth surface and increases in the sensible heat flux into the surface which ultimately heats the surface air.

The reasons that some models simulate the tropical precipitation and subtropical subsidence regimes for the dry Sahara better than others are likely related to the choice of convection scheme and its interactions with the cloud scheme. Such model-specific parameterization difference details are beyond the scope of this study. Since the models that do a better job of simulating the present-day Sahara are more accurately portraying the relevant physical processes for this region, we assume these models are more likely to better simulate future changes in these physical processes. This assumption is difficult to quantify but is common to modeling studies of future climate [*McAvaney et al.*, 2001]. This analysis expands upon Liu2001 in terms of a more consistent multi-model result, and provides a plausible projection of climate change in this region that can be used as a starting point for future analyses with improved models.

2. Data and Definition

Eighteen coupled models with different resolution have eighty-year integrations of control (CTL) and perturbed (PER) in CMIP runs. The CTL runs keep constant external forcing of CO_2 and solar radiation at present-day levels. The PER runs increase CO_2 at one percent per year compound and the concentration doubles at about year seventy. All the model outputs are interpolated to the same resolution as observational data of

2.5°×2.5°. The CTL mean of year 41-80 serves as a reference. Table 1 summarizes basic configurations of each model and their performance to simulate the Sahara dry climatology. Other details are referred to by Covey et al (2001). **Table 1**

Observational and reanalysis data are used to evaluate the ability of the eighteen models to simulate the dry climatology of the Sahara Desert and to select models with better performance. Two sources are IPCC 1°×1°rainfall 1981-90 mean [*New et al.*, 2000] and ECMWF Reanalysis 1979-93 (ERA15). Their climatology over the Sahara is shown in the first two lines of table 1.

There are several definitions of the Sahara Desert [*Tucker*, 1991; *Goudie*, 2000]. We follow Liu2001 to define it as bounded by the 50 mm isoline of mean annual rainfall in the domain of 20°W∼40°E longitude and 15°N∼35°N latitude as in the PCM study (Figure 1). Details of this definition and implications for simulation in a global coupled climate model are given by Liu2001. **Figure 1**

3. Results

IPCC and ERA15 produce a reference dry climatology in the Sahara as shown in the first two rows of table 1. Differences exist between the two sources especially in the total grid number or the dry area. Such differences mainly lie in the Western Sahara as displayed in figure 1. The mean annual precipitation bounded by the 50mm isoline is 20.4mm with a total grid number of 98 corresponding to about $7.6\times10^6\mathrm{Km}^2$. The longitude and latitude means are 11.8°E and 24.1°N respectively.

Table 1 also lists the corresponding statistics for the Sahara interpolated from eighteen CMIP models. Six models are closest to the dry climatology of the two observational

datasets. They are CCSR, CSIRO (abbreviated CSIR subsequently), CSM, GISS, PCM, and UKMO.

Isolines in figure 1 represent the 50 mm mean annual rainfall from the two observations and these six models (all on $2.5^{\circ}\times2.5^{\circ}$grid). The isolines correspond closely in all but the western boundary of the ERA15 and CMAP. The UKMO southern boundary in the central Sahara is farther north than others and it is not selected for future trend study here. In general, the five other models follow that observed in the domain.

The multi-model ensemble means from the CTL and PER runs in the five models are shown in Figure 2. The PER is the mean of years 61-70 near the time of CO_2 doubling. The PER isoline is about 1^{o} latitude further northward both in the northern and southern boundaries than those of CTL. Such a northward shift is consistent with that shown in the PCM runs (Liu2001). The mean two dimensional model displacement of the Sahara boundary is considerably less than the difference between the models' control simulations as in Figure 1.

Figure 2

Since the previously analyzed PCM is included in the multi-model ensemble in Figure 2, we show trends for each model individually in Figure 3 a-e. These plots are 30-year running means of the PER runs minus the CTL forty-year climatologies for each model. The five-model-mean surface net heat fluxes are shown in figure 3f as four 20-year-means since the yearly output for these variables are not available.

Figure 3

In the increasing CO_2 concentration scenario the mean latitude (lat) ends up further north at the time of CO_2 doubling than at the beginning of the simulations in all the models. This is reflected in the multi-model mean in figure 2 and figure 3a. However, within the integrations there is evidence of low frequency variability. In figure 3a the mean

latitude continuously moves northward (increasing positive anomalies) in the first twenty to thirty years (PCM, CSM, and CSIR) or has a small southward shift (CCSR and GISS). After this time period, the Sahara keeps moving north in three models (GISS, CSM and CSIR) while in PCM and CCSR it retreats southward somewhat after year 50 to 55. Generally the multi-model ensemble mean curve (gray) keeps stable at about +0.15°latitude during the first 20 years then moves northward and reaches about 0.55°latitude further north by year 70. Such a northward shift trend is similar to the PCM ensemble runs as shown in figure 4f of Liu2001. The CO_2 modeling experiments have shown an intensification of the hydrological cycle with zonal mean increases in precipitation in the tropics and decrease in the subtropics *Cubasch et al.*, 2001]. The present study shows the regionalization of this result. That is, the West African monsoon is intensifying slightly with more rainfall on the southern boundary of the Sahara (figures not shown), with increased subsidence over the Sahara thus shifting the low precipitation region associated with the Sahara northward.

Another similar trend is the surface temperature shown in figure 3c. The Sahara continuously gets warmer in the five models. CSIR and CCSR produce a much faster warming trend than the other three models. In these two models the Sahara ends up being over 2.1°C warmer than the CTL climatology, while in other three models it is about 1.5°C warmer. The multi-model mean temperature is 1.8°C warmer at the time of CO_2 doubling at year 70.

The five models do not show large trends in the mean longitude (lon), total number (num) of grids with annual rainfall less than 50mm, and mean precipitation (pr). In figure 3b the PCM and GISS show the Sahara moving westward while CSM and CSIR

say the opposite. The CCSR does not agree with other four models and shows a 40-year east-west fluctuating trend. The multi-model ensemble mean generally shows a steady small westward shift of the Sahara.

The Sahara shrinks in CSM, PCM and GISS while it expands in CCSR and CSIR as shown in figure 3d. The multi-model mean area is about 1 grid box ($2.5°\times2.5°$or $77000Km^2$) larger than the CTL climatology. The drying trend in CCSR, CSIR and CSM is more apparent than in PCM and GISS as shown in figure 3e. The multi-model mean drying is about 1 mm/year by year 70.

Three mean surface heat flux components illustrate the processes involved with the mean warming trend and are shown in figure 3f. The multi-model mean net long wave radiation (lgnw) gets more negative (i.e. less net upward longwave and more energy into the surface) and is about -1.5 W/m^2 by the year of 70, while the sensible heat flux (senh) gets more positive (energy leaving the surface) and reaches about 1.2 W/m^2. Not much change occurs in the latent heat flux (ltnt). Though these trends are multi-model ensemble means of four 20-year mean periods, they are consistent with trends in surface temperature in figure 3c. The net surface long wave radiation loss due to the increasing CO_2 and the increased sensible heat flux both act to warm the surface air temperature over the Sahara. From this point of view, the warming over the Sahara for this multi-modeled ensemble is directly related to the enhancement of greenhouse effect as Liu2001 proposed for a single model.

4. Discussion

Five of eighteen coupled models simulate a similar modern dry climatology over the Sahara Desert compared to observational data. They are assumed to provide a plausi-

ble projection of future Sahara trends under the increasing CO_2 concentration scenario. The models project a northward retreating, warming and drying Sahara with increasing CO_2. Such trends agree well with those projected by the PCM ensemble runs with other greenhouse gases increasing simultaneously in a previous analysis (Liu2001). These analyses give a preliminary indication of possible future changes of the Sahara, and provide a starting point for future studies with improved models.

Acknowledgments. This research was partly supported by the Frontier Research System for Global Change through its sponsorship of the International Pacific Research Center (IPRC). A portion of this study was supported by the Office of Biological and Environmental Research, U.S. Department of Energy, as part of its Climate Change Prediction Program. The authors thank Johannes Loschnigg for helpful comments on the manuscript. The National Center for Atmospheric Research is sponsored by the National Science Foundation.

References

Bunting, A. H., Rainfall trends in the West African Sahel, *Q. J. Roy. Met. Soc., 102,* 59-64, 1976.

Charney, J., P. H. Stone, W. J. William, Drought in the Sahara: a biogeophysical feedback mechanism, *Science, 187,* 434-445, 1975.

Covey, C., K. M. AchutaRao, U. Cubasch, P. Jones, S.J. Lambert, M. E. Mann, T. J. Phillips and K.E. Taylor, An overview of results from the Coupled Model Intercomparison Project, Global and Planetary Change, in press.

Cubasch, U., G. A. Meehl, G. J. Boer, R. J. Stouffer, M. Dix, A. Noda, C. A. Senior, S. Raper, and K. S. Yap, Projections of future climate change, in *Climate change 2001: the scientific basis*, edited by J. T. Houghton et al., pp 944, Cambridge, 2001.

Dumont, H. J., Neolithic hyperarid period preceded the present climate of the central Sahel, *Nature, 274,* 356-358, 1978.

Goudie, A., *The Human Impact on the Natural Environment (5th ed.)*, pp 511, Cambridge, MA: MIT Press, 2000.

Gasse, F., R. Tehet, A. Durand, E. Gibert, J. G. Fontes, The arid-humid transition in the Sahara and the Sahel during the last deglaciation, *Nature, 346,* 141-146, 1990.

Greenhut, G. K., Comparison of temperature gradient model predictions with recent rainfall trends in the Sahel, *Mon. Wea. Rev., 109,* 137-147, 1981.

Klaus, D., Spatial distribution and periodicity of mean annual precipitation south of the Sahara, *Archiv fur Met., Geophy., und Biok., Ser. B, 26,* 17-27, 1978.

Littmann, T., Rainfall, temperature and dust storm anomalies in the African Sahel, *Geo. J., 157,* 136-160, 1991.

Liu, P., G. Wu, and S. Sun, Local meridional circulation and deserts, *Adv. Atm. Sci., 18,* 864-872, 2001a.

Liu, P., W. M. Washington, G. A. Meehl, G. Wu, and G. L. Potter, Historical and future trends of the Sahara Desert, *Geo. Res. Lett, 28,* 2683-2686, 2001b.

Maley, J., Palaeoclimates of central Sahara during the early Holocene, *Nature, 269,* 573-577, 1977.

McAvaney, B. J., C. Covey, S. Joussaume, V. Kattsov, A. Kitoh, W. Ogana, A. J. Pitman, A. J. Weaver, R. A. Wood, and Z.-C. Zhao, Model evaluation, in *Climate change 2001:*

the scientific basis, edited by J. T. Houghton et al., pp 944, Cambridge, 2001.

Meehl, G. A., G. J. Boer, C. Covey, M. Latif, and R. J. Stouffer, The Coupled Model Intercomparison Project (CMIP). *Bull. Amer. Meteorol. Soc.*, *81*, 313-318, 2000.

New, M. G., M. Hulme and P. D. Jones, Representing twentieth century space-time variability. II: Development of a 1901-1996 mean monthly terrestrial climate fields, *J. Clim., 13,* 2217-2238, 2000.

Palmer, T. N., Influence of the Atlantic, Pacific, and Indian oceans on Sahel rainfall, *Nature, 322,* 251-253, 1986.

Ritchie, J. C., C. H. Eyles, and C. V. Haynes, Sediment and pollen evidence for an early to mid-Holocene humid period in the eastern Sahara, *Nature, 314,* 352-355, 1985.

Tucker, C. J., H. E. Dregne, and W. W. Newcomb, Expansion and concentration of the Sahara Desert from 1980 to 1990, *Science, 253,* 299-301, 1991.

Washington, W. M., J. W. Weatherly, G. A. Meehl, A. J. Semtner Jr., T. W. Bettge, A. P. Craig, W. G. Strand Jr., J. Arblaster, V. B. Wayland, R. James, and Y. Zhang, Parallel climate model (PCM) control and transient simulations, *Clim. Dyn., 16,* 755-774, 2000.

Wolter, K., Modes of tropical circulation, Southern Oscillation, and Sahel rainfall anomalies, *J. Clim., 2,* 149-172, 1989.

Zeng, N., J. D. Neelin, K.-M. Lau and J. Tucker, Enhancement of interdecadal climate variability in the Sahel by vegetation interaction, *Science, 286,* 1537-1540, 1999.

Table 1. CMIP Model Configuration and CTL Run for Sahara

Model	Orig. AGCM Resolution	CO_2 PPM	Solar Cons. W/m^2	Grids[a,b] No.	Rain[a] mm/yr	Long.[a] °E	Lat.[a] °N	Selected
ERA15	2.5°×2.5°			109	20.2	12.0	24.3	
IPCC	1°×1°			87	20.6	11.5	23.9	
mean				98	20.4	11.8	24.1	
BMRC	R21[c]L9	330	1365	196	5.7	11.7	23.9	No
CCC	T32[c]L10	330	1370	0				No
CCSR	T21[c]L20	345	1365	109	30.4	7.8	25.6	Yes
CERF	T21L30	353	1370	14	44.6	33	25.2	No
CSIR	R21L19	330	1367	123	17.3	12.9	23.6	Yes
CSM	T42[c]L18	355	1367	95	17.7	13.9	24.5	Yes
ECH3	T21L19	345	1365	153	15.9	12.5	24.4	No
ECH4	T42L19	240	353	54	24.5	21.9	24.7	No
GFDL	R30[c]L9	360	1365	0				No
GISS	4[o]×5[o]L9	315	1367	73	20.4	16.3	25.6	Yes
IAP	R15[c]L9	345	1367	3	48.3	30	25	No
LMD	3.6[o]×3.8[o]L15	320	1367	3	43.1	-15.8	24.2	No
MRI	4[o]×5[o]L15	345	1365	53	34.6	0.1	23.5	No
NRL	T47[c]L18			131	9.3	11.8	23.3	No
PCM	T42L18	355	1367	83	17.2	11	25.3	Yes
UKMO	2.5[o]×3.75[o]L19	322.6	1365	102	25.1	14.2	24.4	No
UKMO3	2.5[o]×3.75[o]L19	289.6	1365	48	29.4	24.9	24.7	No
WM	R15L9			0				No

[a] Interpolated 50mm isoline bounded mean.

[b] one 2.5°×2.5°∼77000Km^2.

[c] R21∼3.2°×5.6°; T32∼3.8°×3.8°; T21∼5.6°×5.6°; T42∼2.8°×2.8°; R15∼4.5°×7.5°; T47∼2.5°×2.5°

Figure 1. Climatological rainfall isolines of 50 mm covering the Sahara Desert from eight data sources. Unit: mm/year.

Figure 2. Trend of the Sahara bounded by five model mean climatological 50 mm annual rainfall isoline (black: CTL year 41 to 80; gray: PER year 61 to 70)

Figure 3. Five model simulated 30-year running mean trends of the Sahara averaged as a whole. a-e are deviations from PER relative to CTL mean. They are average latitude, longitude, surface temperature, number of grids, and annual rainfall respectively. f are mean surface net heat fluxes with lgnw as long wave, ltnt as latent heat, and senh as sensible heat.

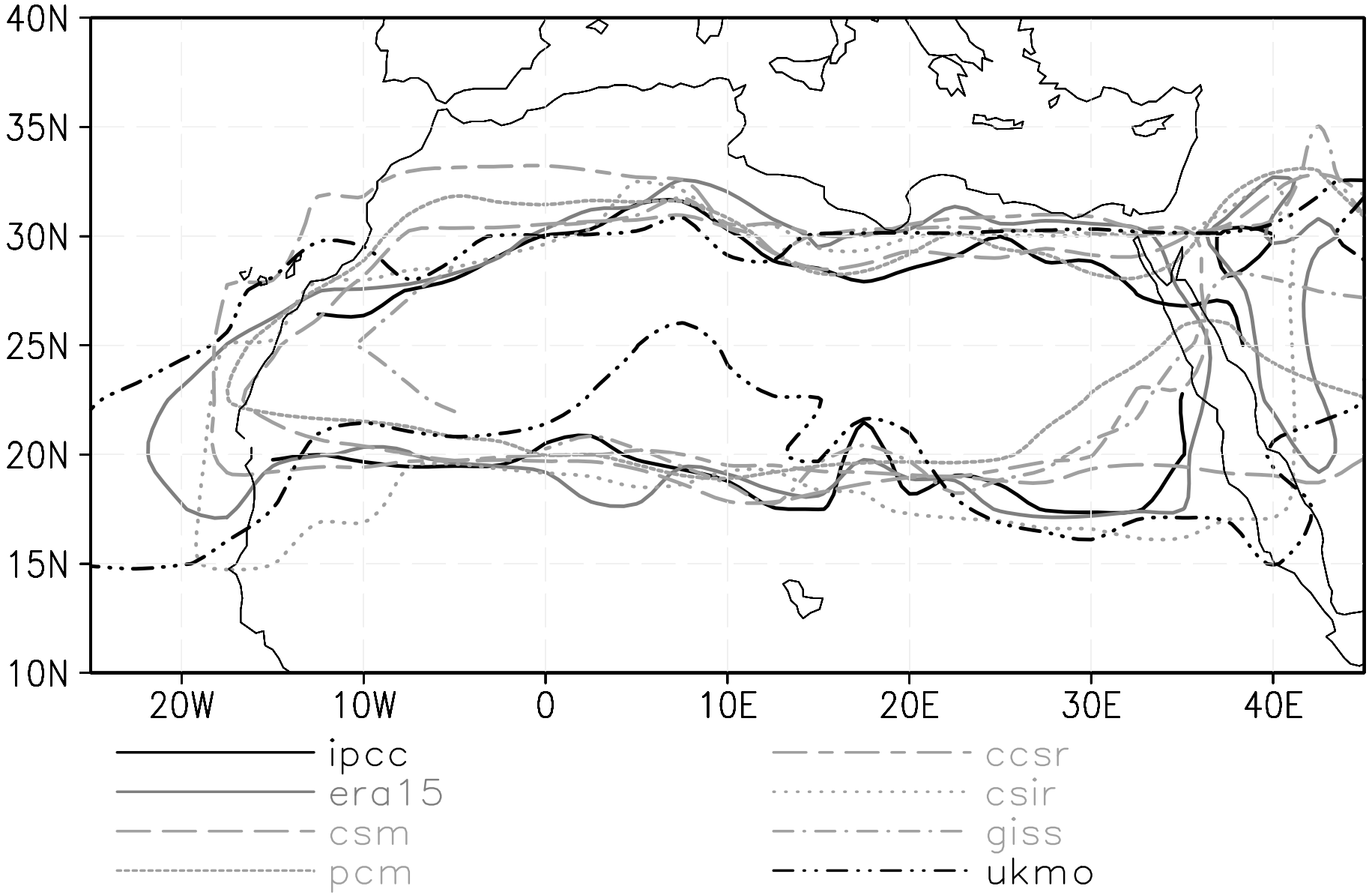
40N
35N
30N
25N
20N
15N
10N
20W
10W
0
10E
20E
30E
40E
ipcc
era15
csm
pcm
ccsr
csir
giss
ukmo

Fig. 1

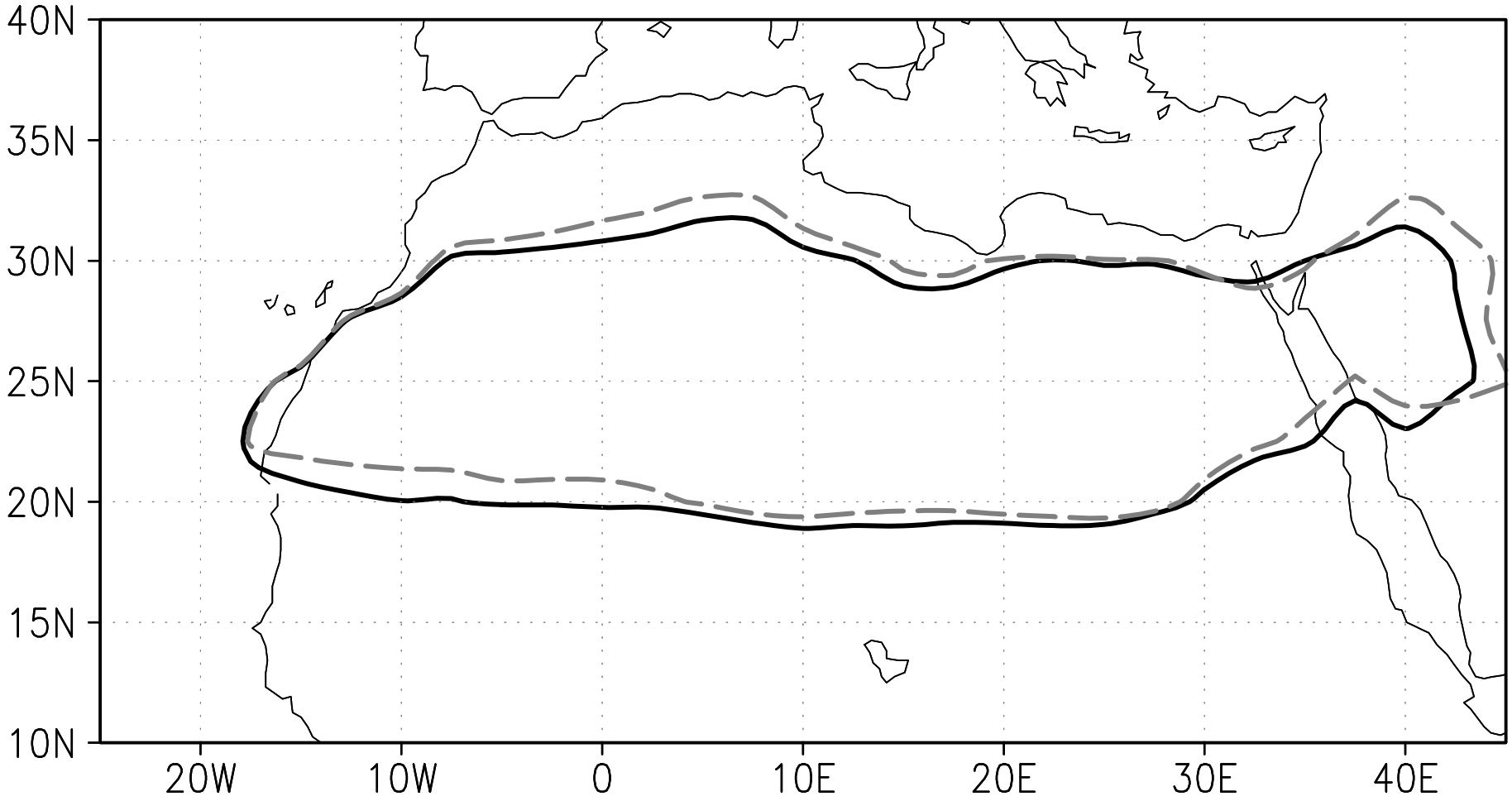

Fig. 2

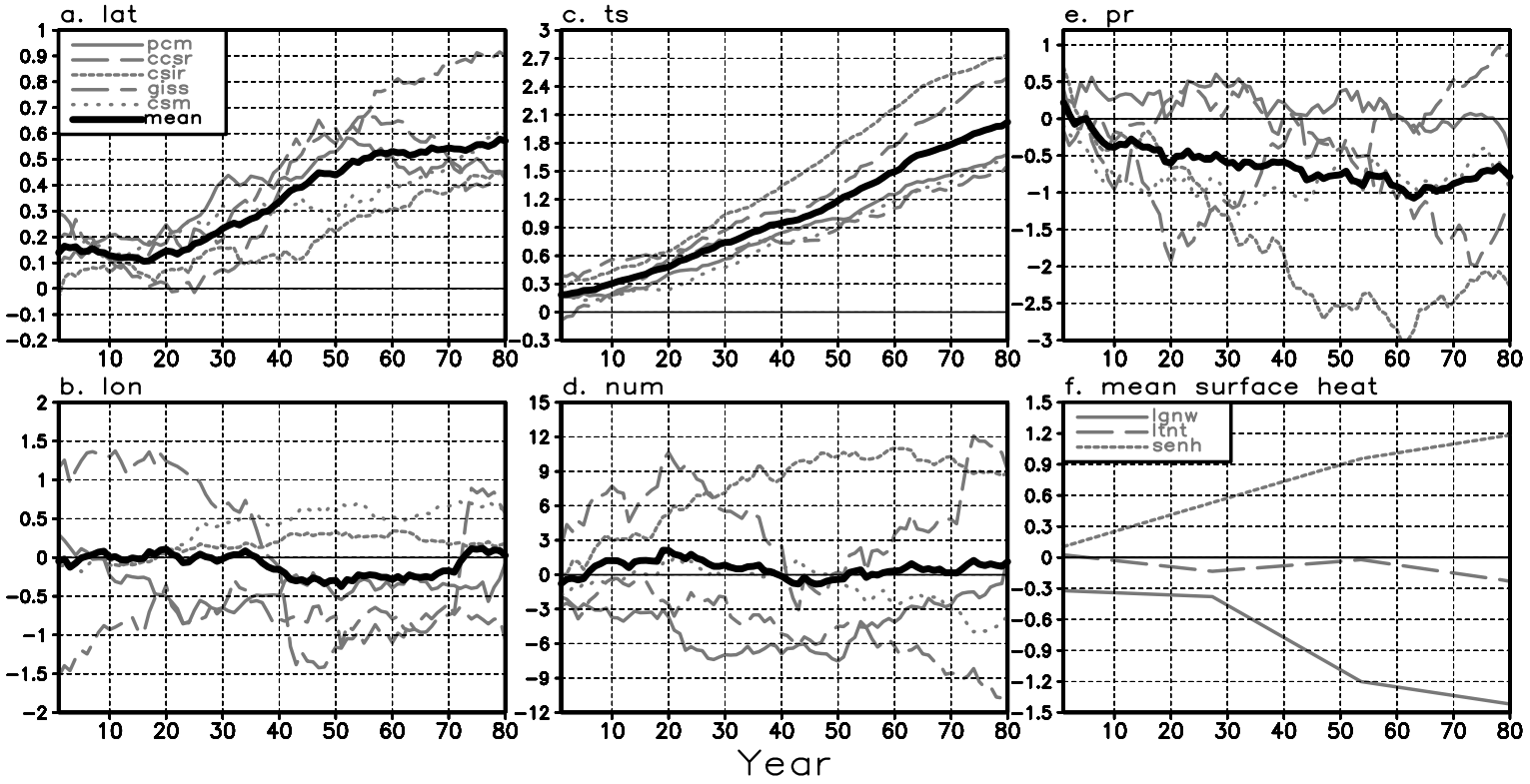
a. lat
pcm
ccsr
csir
giss
csm
mean
c. ts
e. pr
b. lon
d. num
f. mean surface heat
lgnw
lnt
senh
Year

Fig. 3